PRECLINICAL REPORTS

# Fractional $CO_2$ laser ablation leads to enhanced permeation of a fluorescent dye in healthy and mycotic nails—An imaging investigation of laser–tissue effects and their impact on ungual drug delivery

Vinzent Kevin Ortner MD[1]  |  Nhi Nguyen MSc[1,2]  |  Jonathan R. Brewer PhD[2]  |
Vita Solovyeva PhD[2,3]  |  Merete Haedersdal MD, PhD, DMSc[1]  |
Peter Alshede Philipsen PhD[1]

[1]Department of Dermatology, Copenhagen University Hospital, Bispebjerg and Frederiksberg, Copenhagen, Denmark

[2]Department of Biochemistry and Molecular Biology, University of Southern Denmark, Odense, Denmark

[3]Faculty of Mathematics and Science, University of Oldenburg, Oldenburg, Germany

**Correspondence**
Vinzent Kevin Ortner, MD, Department of Dermatology and Wound Healing Centre, Copenhagen University Hospital, Bispebjerg and Frederiksberg, Nielsine Nielsens Vej 17, Entrance 9, 2nd floor, 2400 Copenhagen NV, Denmark.
Email: vinzent.kevin.ortner@regionh.dk

## Abstract

**Purpose:** Conventional oral antifungal therapies for onychomycosis (OM) often do not achieve complete cure and may be associated with adverse effects, medical interactions, and compliance issues restricting their use in a large group of patients. Topical treatment can bypass the systemic side effects but is limited by the physical barrier of the nail plate. Ablative fractional laser (AFL) treatment can be used to improve the penetration of topical drugs into the nail. This study visualized the effects of laser ablation of nail tissue and assessed their impact on the biodistribution of a fluorescent dye in healthy and fungal nail tissue.

**Methods:** For the *qualitative* assessment of $CO_2$ AFL effects on healthy nail tissue, scanning electron microscopy (SEM), coherent anti-Stokes Raman scattering microscopy (CARS-M), and widefield fluorescence microscopy (WFM) were used. To *quantitate* the effect of laser-pretreatment on the delivery of a fluorescent dye, ATTO-647N, into healthy and fungal nail tissue, ablation depth, nail plate thickness, and ATTO-647N fluorescence intensity in three nail plate layers were measured using WFM. A total of 30 nail clippings (healthy $n = 18$, fungal $n = 12$) were collected. An aqueous ATTO-647N solution was directly applied to the dorsal surface of 24 nail samples (healthy $n = 12$, fungal $n = 12$) and incubated for 4 hours, of which half (healthy $n = 6$, fungal $n = 6$) had been pretreated with AFL (30 mJ/mb, 15% density, 300 Hz, pulse duration <1 ms).

**Results:** Imaging revealed a three-layered nail structure, an AFL-induced porous ablation crater, and changes in autofluorescence. While intact fungal samples showed a 106% higher ATTO-647N signal intensity than healthy controls, microporation led to a significantly increased fluorophore permeation in all samples ($p < 0.0001$). AFL processing of nail tissue enhanced topical delivery of ATTO-647N in all layers, (average increase: healthy +108%, fungal +33%), most pronounced in the top nail layer (healthy +122%, fungal +68%). While proportionally deeper ablation craters correlated moderately with higher fluorescence intensities in healthy nail tissue, fungal samples showed no significant relationship.

**Conclusion:** Fractional $CO_2$ laser microporation is a simple way of enhancing the passive delivery of topically applied ATTO-647N. Although the impaired nail

plate barrier in OM leads to greater diffusion of the aqueous solution, AFL can increase the permeability of both structurally deficient and intact nails.

# INTRODUCTION

Onychomycosis (OM), the fungal infection of the nail unit, comprises more than half of all nail disorders and 30% of cutaneous fungal infections.[1] With a rising prevalence of over 5.5%, a high recurrence rate of up to 20%, a reported decrease in quality of life, and potentially severe long-term complications including acute bacterial cellulitis, OM constitutes a major public health concern.[2–8]

Despite the unfavorable side-effect profile of systemic antifungal medication,[9] OM often requires oral treatment owing to the low efficacy of topical treatment options and limited indication of laser devices (Table S1). Consequently, the concept of device-assisted pretreatment for penetration enhancement is rapidly gaining interest as a way of increasing the efficacy of topical formulations. Ablative fractional lasers (AFL) can create an array of microscopic laser channels while keeping surrounding tissue intact. Recent studies have succeeded in using AFL as a method of pretreatment to enhance topical delivery into healthy nail tissue.[10] While the majority of clinical laser-assisted drug delivery studies have been conducted on skin conditions, there is a mounting body of evidence, summarized in Table 1, supporting the use of AFL as a penetration enhancer for topical treatment of nail disease.[11,12] In-depth knowledge of the nail plate structure and laser–tissue interactions is crucial for understanding the challenges diseased nails pose to light-based treatments and topical drug delivery.[13] Clinical empirical evidence on the application and utility of AFL as pretreatment for enhanced efficacy of topical antifungals for treatment of OM has outpaced preclinical investigations. While laser-assisted ungual delivery (LAUD) has been evaluated in healthy nail tissue, a comparative investigation and visualization of a topically applied model drug in ex vivo fungal and healthy nail tissue to determine the effect of AFL pretreatment for enhanced transungual delivery is lacking.

This study evaluated the distribution pattern and signal intensity of a fluorescent dye following laser-pretreatment of both healthy and fungal toenails using widefield fluorescence microscopy (WFM). The objective of this study was to investigate the effects of AFL on drug delivery in both healthy and diseased nail tissue. As a preliminary step, the effects of fractional $CO_2$ laser ablation of healthy nail tissue were investigated using scanning electron microscopy (SEM), coherent anti-Stokes Raman scattering microscopy (CARS-M), and WFM, and compared to previous investigations.[13,37] Following that, the signal intensity of a topically applied fluorescent tracer dye, ATTO-647N, was measured on WFM images of healthy and fungal nail samples with and without AFL processing. By visualizing the laser–tissue effects and quantitating their impact on the diffusion of topically applied compounds in healthy and fungal nail tissue, this study tried to provide a deeper understanding of LAUD to further refine this technique.

# MATERIALS AND METHODS

## Study setup

To *qualitatively* demonstrate the effect of an ablative fractional $CO_2$ laser (DeepFX, UltraPulse CO2, Lumenis; $\lambda = 10{,}600$ nm) on the micromorphology of healthy nail plate tissue, we used SEM, CARS-M, and WFM. For the *quantitative* assessment of AFL poration and ATTO-647N fluorescence intensity, WFM images of healthy and mycotic samples were captured.

## Tissue specimens and processing

For the initial investigation of laser–tissue effects, fingernail clippings ($n = 3$) from two healthy, volunteers (Caucasian male, aged 26 and 51), were clipped, cleaned, and treated with a single pass of AFL (80 mJ/mb, 5% density). The image acquisition and image analysis were performed at the Danish Molecular Biomedical Imaging Center (DaMBIC, University of Southern Denmark).

For the transungual delivery investigation, nail samples from healthy participants ($n = 18$) and anonymous discard clippings from patients with microscopy-verified fungal nail disease ($n = 12$) from the Department of Dermatology at the Copenhagen University Hospital in Denmark were collected. Direct microscopy was performed on anonymous samples incubated with an optical whitening agent, Blankophor, for 30 minutes to detect fluorescent fungal elements (hyphae, pseudohyphae, or spores) as part of routine diagnostics.[38] The edges of the nail samples were trimmed to reduce their curvature and flatten the surface to facilitate a perpendicular beam impact before cleaning with deionized water. The nail clippings were patted dry before undergoing laser ablation and treated in one batch to avoid

**TABLE 1** Overview of studies on clinical and preclinical laser-assisted drug delivery in healthy and diseased nail tissue

| Year and author | Sample size | Condition | Compound | MW (g/mol) | Vehicle | Application | Laser type and device | Settings | Density |
|---|---|---|---|---|---|---|---|---|---|
| 2013 EH Lim[14] | 2 | Onychodystrophy | Desoximetasone 0.25% | 376.4 | Lotion | Once daily | CO2 (10,600 nm); Mosaic eCO2, Lutronic | 160 mJ (3 passes) | 150 spots cm$^{-2}$ |
| 2013 OO[c] Morais[15a] | 9 | Onychomycosis | Amorolfine 5% | 317.5 | Lacquer | Once weekly | Er:YAG (2,940 nm); Etherea, Industra | 50 mJ mtz$^{-1}$ (number of passes dependent on nail thickness and patient tolerability) | N.A. |
| 2014 EH Lim[16] | 24 | Onychomycosis | Amorolfine 5% | 317.5 | Cream | Once daily | CO2 (10,600 nm); Mosaic eCO2, Lutronic | 160 mJ (2–3 passes) | 150 spots cm$^{-2}$ |
| 2015 GB deOliveira[17] | 7 | Onychomycosis | MAL 16% | 181.6 | Cream | Before PDT | CO2 (10,600 nm); – | 160 mJ (3 stacks) | 600 μm spacing between mtz |
| 2015 AK Bhatta[18] | 75 | Onychomycosis | Terbinafine 1% | 291.4 | Cream | Once daily | CO2 (10,600 nm); 2030CI, Wuhan Qi Zhi Laser Technology | 99 mJ (2–6 passes) | 410 spots cm$^{-2}$ |
| 2016 BR Zhou[19] | 60 | Onychomycosis | Luliconazole 1% | 354.3 | Cream | Once daily | CO2 (10,600 nm); AcuPulse, Lumenis | 10–15 mJ (1–3 stacks) | 10% |
| 2016 J Zhang[20] | 9 | Onychomycosis | Amorolfine 5% | 317.5 | Lacquer | Twice weekly | Er:YAG (2,940 nm); Sciton | 35–62 J cm$^{-2}$ (3 passes) | 120 spots cm$^{-2}$ |
| 2017 J Shi[21] | 31 | Onychomycosis | Terbinafine 1% | 291.4 | Cream | Once daily | CO2 (10,600 nm); AcuPulse; Lumenis | 15 mJ (multiple passes) | 15% |
| 2017 A Koren[22] | 54 | Onychomycosis | (a) ALA 20% (b) Amorolfine 5% | (a) 167.6 (b) 317.5 | (a) Cream (b) Lacquer | (a) Before PDT (b) Once weekly | CO2 (10,600 nm); Lumenis Ultrapulse | 150 mJ (single pass) | 3% |
| 2018 EB Abd El-Aal[23] | 102 | Onychomycosis | (a) Tazarotene 0.1% (b) Tioconazole 28% | (a) 351.5 (b) 387.7 | (a) Gel (b) Solution | Once daily | CO2 (10,600 nm); Smartxide DOT, DEKA, Italy | Power 10 W (3 stacks) | 700 μm spacing between mtz |

(Continues)

**TABLE 1** (Continued)

| Year and author | Sample size | Condition | Compound | MW (g/mol) | Vehicle | Application | Laser type and device | Settings | Density |
|---|---|---|---|---|---|---|---|---|---|
| 2019 RA El-Tatawy[24] | 30 | Onychomycosis | Tioconazole 28% | 387.7 | Lacquer | Twice daily | CO2 (10,600 nm); Smartxide DOT, DEKA, Italy | Power 11–15 W (1–3 stacks, 1–3 passes) | 500 μm spacing between mtz |
| 2020 M Abdallah[25] | 21 | Onychomycosis | Methylene Blue 2% | 319.9 | Solution | Before PDT | CO2 (10,600 nm); Fire-xel scanner system, Bison | 180 mJ (3 stacks, 2 passes) | 500 μm spacing between mtz |
| 2020 B Rajbanshi[26] | 160 | Onychomycosis | Terbinafine 1% | 291.4 | Ointment | Once daily | CO2 (10,600 nm); Wuhan Miracle Laser Co., Ltd. | No fixed setting (dependent on heat sensation) | 1000–1500 μm spacing between mtz |
| 2020 AM Zaki[27] | 120 | Onychomycosis | Tioconazole 28% | 387.7 | Solution | Twice daily | CO2 (10,600 nm); SmartXide Square, DEKA, Florence, Italy | Power of 10–15 W (according to nail thickness), 3 stacks, pulse duration of 500 μs | 700–800 μm spacing between mtz |
| 2021 J Zhang[28] | 78 | Onychomycosis | Amorolfine 5% | 317.5 | Lacquer | Twice weekly | Er:YAG (2,940 nm); Sciton | 35–60 J cm$^{-2}$ (dependent on nail thickness and patient tolerability) | 120 spots cm$^{-2}$ |
| 2021 W Shehadeh[29] | 22 | Nail psoriasis | Calcipotriol 50 μg/g + Betamethasone 0.5 mg/g | 392.5 + 412.6 | Gel | Once daily | CO2 (10,600 nm)[b]; Ultrapulse Encore, Lumenis Ltd. | 60–110 mJ (dependent on patient tolerability) | 3% |
| 2021 N Essa Abd Elazim[30] | 27 | Nail psoriasis | Tazarotene 0.1% | 351.5 | Gel | Once daily | CO2 (10,600 nm); Daeshin Enterprise Co., Ltd. Model: Multixel | 140 mJ 2–3 passes | 150 spots cm$^{-2}$ |
| 2014 CH Yang[31] | 1 | Healthy | Saline | 58.4 | Solution | Once (<5 min) | CO2 (10,600 nm); UltraPulse Encore Active FXTM; Lumenis | 20–50 mJ | 10% |

**TABLE 1** (Continued)

| Year and author | Sample size | Condition | Compound | MW (g/mol) | Vehicle | Application | Laser type and device | Settings | Density |
|---|---|---|---|---|---|---|---|---|---|
| 2016 MT Tsai[32] | 3 | Healthy | Sulconazole 1% | 460.8 | (a) Solution (b) Cream | Once (<5 min) | CO2 (10,600 nm); UltraPulse Encore Active FXTM | 20–50 mJ | N.A. |
| 2017 S Vanstone[13] | 3 | Healthy | Caffeine 20 mg/mL | 194.2 | Solution | Once (72 h) | YDFL (532 nm)[c]; Fianium FP-1060-5-FS | 31–250 mJ pore$^{-1}$ | 500 spots cm$^{-2}$ |
| 2019 AV Belikov[33] | N.A. | Healthy | Methylene Blue 0.5%–3% | 319.9 | Gel | Before irradiation (dual stage LADD) | Er:YLF (2,810 nm); — | 3.9–4.1 mJ | N.A. |
| 2019 I Sveikauskaite[34] | N.A. | Healthy | (a) Amorolfine 5% (b) Amorolfine 5% + Thioglycolic acid 5% (c) Amorolfine 5% + Urea 5% | (a) 317.5 (b) +92.1 (c) +60.6 | Lacquer | Once (24 h) | CO2 (10,600 nm); Candela CO2RE laser, Syneron Candela, Wayland, MA, USA | 50–80 mJ | N.A. |
| 2020 I Sveikauskaite[35] | N.A. | Healthy | (a) Naftifine 5% (b) Naftifine 5% + Thioglycolic acid 5% (c) Naftifine 5% + Salicylic acid 0.5% | (a) 323.9 (b) +92.1 (c) +138.1 | Lacquer | Once (24 h) | CO2 (10,600 nm); Candela CO2RE laser, Syneron Candela, Wayland, MA, USA | 50–80 mJ | N.A. |
| 2021 AV Belikov[36] | 5 | Healthy | Methylene Blue 0.001% | 319.9 | Solution | Before irradiation (dual stage LADD) | Er:YLF (2,810 nm); — | 1–4 mJ | N.A. |

Abbreviations: ALA, 5-Aminolevulinic acid; LADD, laser-assisted drug delivery; MAL, methyl aminolevulinate; mtz, microthermal zone.

[a]Protocol only; study results published as thesis.

[b]plus 595-nm PDL (Perfecta, Syneron-Candela) on nail folds.

[c]Ytterbium-doped fiber laser with frequency doubling lithium triborate crystal.

hydration-dependent variation in laser–tissue interaction. Half of the fungal samples as well as nine healthy clippings ($n = 15$) were anchored at their lateral edge with adhesive tape to a styrofoam board and processed with the same AFL device (30 mJ/mb, 10% density, 300 Hz frequency, fixed pulse duration <1 ms). Twenty-four samples were labeled with a tracer dye solution as described below. All thirty samples were embedded in optimal cutting temperature medium (Tissue TEK OCT) before sectioning on a microtome-cryostat (Leica CM 3050S) at fixed temperatures (20°C in the chamber and −15°C for the specimen). To avoid tissue tears, samples were sectioned transversally in parallel to the fiber direction of the intermediate layer and the free edge of the nail plate[39] at a thickness of 10 μm. For each nail sample, nine cryosections were prepared ($n = 270$).

## Scanning electron microscopy

SEM enables high-resolution examination of surfaces by scanning them with a focused beam of electrons and detecting the emission of secondary electrons. This electron microscopy method can be used to study the topography of solid tissues and ultrastructure of laser–tissue effects.[40] To visualize and characterize the surface texture of nail tissue after AFL processing, SEM (FEI Quanta 200) imaging of unsectioned nail clippings was performed at an accelerating voltage of 10 kV in high vacuum mode. As nail tissue is not considered beam- or vacuum-sensitive, gold sputter coating was omitted.

## Coherent anti-Stokes Raman scattering microscopy

CARS-M is a label-free chemically specific imaging technique capable of generating image data based on tissue-intrinsic molecular vibrations, directly visualizing water and lipid content.[41] While conventional microscopic imaging techniques fail to directly visualize molecules in the tissue, CARS-M can visualize specific molecules such as water and lipids in tissue.[42] To describe the influence of AFL on nail tissue composition, CARS-M (Leica TCS SP8 microscope with a ×40 IRAPO objective) was performed with a laser tuned in on OH and CH-group stretching vibrations to visualize water (3260 cm$^{-1}$) and lipid (2850 cm$^{-1}$) content, respectively. The laser used was a picoemerald (APE) with a Stokes beam at 1064 nm, and a pump beam at for lipids 816.4 nm and 790 nm for water. The CARS-M signal was detected using an epi-detector with a short pass filter (Multiphoton-emitter HC 770/SP) to block the lasers and a bandpass filter at 661/11 BrightLine HC for the lipids, and at 620/14 BrightLine HC for the water. The filters were acquired from AHF Analysentechnik.

## ATTO-647N labeling

ATTO-647N is a hydrophilic cationic fluorescent label (MW 746 g/mol) with a high quantum yield in the red spectral region (λex = 646 nm, λem = 664 nm) (Atto-TEC GmbH). In addition, ATTO-647N has been shown not to bind to keratin, that is, better odds of faster distribution.[43] For this study, a 100 μM aqueous solution of the carboxy derivative of ATTO-647N in dimethyl sulfoxide (DMSO), a penetration enhancer, and phosphate-buffered saline (PBS) was prepared (500 μM stock solution in DMSO diluted in PBS to 100 μM). Following cleaning with deionized water, 24 samples (healthy: $n = 12$, fungal: $n = 12$; half of both groups AFL-pretreated) were placed on PBS-soaked gauze. A droplet of the ATTO-647N solution was applied to the dorsal surface of intact and AFL-pretreated nails, and incubated for 4 hours in the dark on top of PBS-soaked gauze. The excess staining agent was removed by washing the nail samples for 2 minutes with PBS.

## Widefield fluorescence microscopy

The cryo-sections were placed on glass slides (Superfrost) and stored at −20°C until inspected under an inverted widefield fluorescence microscope (Olympus IX70. Fluorescence Microscope, Olympus Denmark A/S) equipped with a xenon lamp at 10-fold magnification using a UV-filter cube (λex: 375/28 nm, λem: beam splitter 415 nm λem 460/50 nm, exposure time of 150 ms) to capture morphological images and a custom-made filter cube for ATTO-647N fluorescence (λex:640/30 nm, λem: beam splitter 660 nm, λem: 690/50 nm, exposure time of 10 ms) in a room with dim green light to avoid photobleaching.

The stability of the excitation light was monitored before each microscopy session by an external power meter and fluorescence measurements on a fluorescent plastic standard slide (Chroma Technology, Corp.). The power of the light source proved stable during the sampling process (±10%). Standard measurements showed no significant variation in illumination.

## Image analysis

All images were analyzed using FIJI (ImageJ 1.49, NIH[44]). SEM and CARS-M images were assessed qualitatively. On UV-WFM images, nail plate thickness and depth of AFL-micropores were measured and evaluated for nail dystrophy signs. Nail plate thickness was measured as the shortest distance between dorsal and ventral layer. Micropores were defined as the absence of tissue-corresponding signal. In cross-sectional images, micropores were observed to be of triangular or semi-elliptical shape. The degree of poration describes the relationship between the depth of an ablation crater

**FIGURE 1** Scanning electron microscopy image of healthy nail tissue exposed to 80 mJ/mb of ablative fractional CO2 laser (left: side view, right: top view). Images show complete poration of the nail plate and porous surface structure of the ablation zone
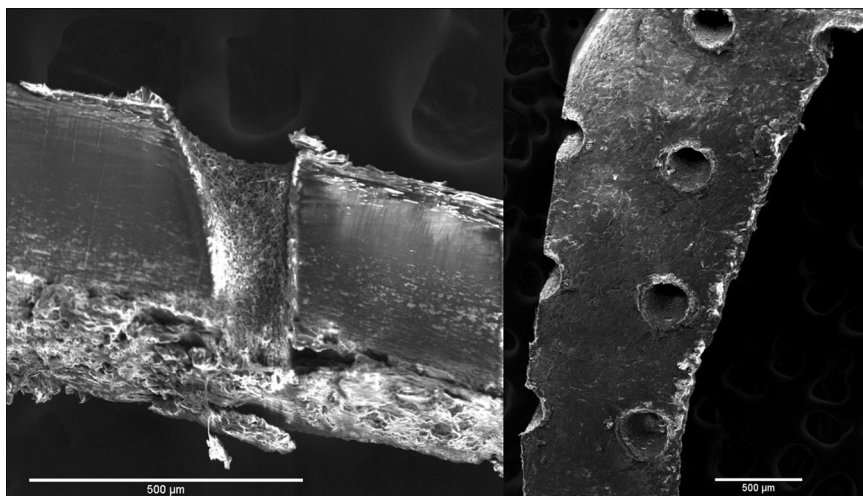


and the thickness of the treated tissue, where complete poration (100%) represents ablation to a depth corresponding to the total thickness of the nail plate. The morphometric assessment of laser-processed nail tissue has been described in detail in our previous publication.[45] Fluorescence signal intensity in ATTO-647N-WFM images was quantitated in a standardized manner by drawing a line with a width of 100 pixels horizontally across the displayed nail sample in three regions of interest: the dorsal, the intermediate, and the ventral layer of the sample.

## Statistics

Based on a significant Levene's test, nonparametric analysis using Kruskal–Wallis and paired Wilcoxon rank tests with Hochberg correction for multiple comparisons were conducted. By calculating the Pearson correlation coefficient ($r$), the linear association between fluorescence intensity and poration depth was explored. Data were visualized using grouped boxplots and scatterplots. Statistical evaluation and data visualization were performed using R and the ggplot2 package in R Studio.

## RESULTS

Microscopy images were assessed *qualitatively* for the micromorphology of laser–tissue effects and nail plate ultrastructure. *Quantitatively*, morphometric dimensions of AFL micropores and ATTO-647N fluorescence signal intensities were measured.

## Morphology and morphometry

SEM images of healthy nail tissue displayed a scale-like dorsal nail surface with an elevated rim-like structure surrounding the laser pore (Figure 1). A highly porous channel structure resembling a truncated cone connected the slightly larger dorsal aperture with the ventral surface opening. Nail tissue revealed nonconductive properties, resulting in electron accumulations on its surface, thereby creating charging artifacts that can mask the trilaminar structure.

Using CARS-M, however, the nail could be clearly subdivided into three distinct layers based on their water/lipid content, consistent with reported thickness relation (3:5:2) in literature (Figure 2). Rim-like structures surrounding the laser channels, corresponding to coagulated keratin, did not exhibit any lipid signal, providing evidence for a potential break-down of lipids following AFL-processing. Strong green-blue autofluorescent signal stemming from the laser-channel surface and naturally occurring autofluorescent signals were only visible at the surface of the nail plate, both ventral and dorsal sides. After AFL-processing, the pore surface and the ventral bottom layer also displayed a substantial increase in autofluorescence in WFM images.

Fluorescence microscopy of untreated healthy controls and laser-treated healthy controls without ATTO-647N labeling resulted in equally low red background fluorescence. While we observed an increase in autofluorescence around the ablation crater, this peak in signal intensity was strictly limited to a thin rim of coagulated tissue. Morphometric measurements of the nail plate thickness and the ablation crater depth based off UV-WFM images are summarized in Table 2. Average nail plate thickness was lower in healthy samples (372 μm; SD 75 μm) than in fungal nails (607 μm; SD 163 μm). The mean ablation depth (unlabeled healthy: 163 μm [SD 53 μm], ATTO-647N-labeled healthy: 199 μm [SD 56 μm], ATTO-647N-labeled fungal: 195 μm [SD 59 μm]) was not influenced by fungal infection but showed high variation resulting in correspondingly inconsistent degree of poration (SD > 15%). Signs of nail plate dystrophy (as illustrated in Figure 3),
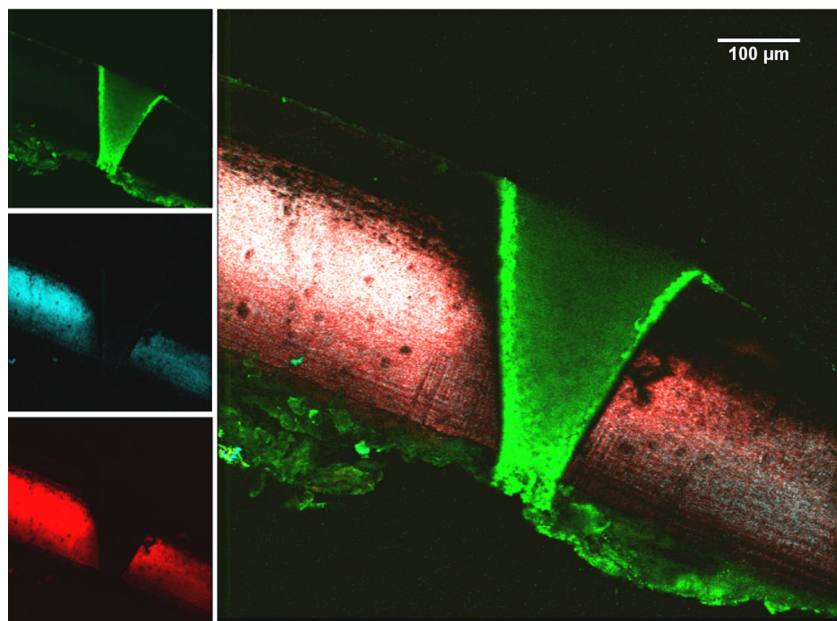
**FIGURE 2** Coherent anti-Stokes Raman scattering microscopy image of a nail plate following 80-mJ/mb AFL processing. While autofluorescence (top left, green pseudocolor) is seen mainly in the laser channel as well as the thermally affected ventral nail layer and the surface of the dorsal layer, the water (mid-left, blue pseudocolor) and lipid (bottom left, red pseudocolor) content are restricted to the middle portion of the nail plate. The overlay (right) shows a trilaminar structure. AFL, ablative fractional laser

and autofluorescence intensities higher than those found in healthy tissue were visible in all fungal samples.

## ATTO-647N delivery

AFL processing led to enhanced uptake and distribution of ATTO-647N, with significantly higher signal intensity in laser-treated healthy (mean 308.2 AU [SD 248.8 AU] and fungal nail samples (mean 428.1 AU [SD 421.8 AU] ($p < 0.0001$) compared to their untreated controls (healthy: mean 146.3 AU [SD 68.6 AU], fungal: mean 305.4 [SD 307.5 AU]) (Table 3). However, unprocessed fungal samples also exhibited stronger significantly ATTO-647N fluorescence ($p < 0.0001$) than healthy controls (Table 4). There was no significant difference in signal intensity between AFL-processed healthy and unprocessed fungal nail tissue ($p = 0.09$), resulting in similar increase in ATTO-647N fluorescence compared with unprocessed healthy samples (+108% vs. 106%, respectively). While AFL processing resulted in improved penetration of ATTO-647N in mycotic samples (top layer +69%, middle layer +16%, bottom layer +13%), the effects were more pronounced in healthy nail tissue (top layer +122%, middle layer +100%, bottom layer +102%).

Delivery of the model drug followed a consistent pattern of marked accumulation on the dorsal surface and predominantly lateral diffusion in the proximity of ablation craters. Figure 4 shows ATTO-647N fluorescence intensity to increase in both healthy and fungal samples after AFL pretreatment, with the most pronounced enhancement in the top layer (Tables 5 and 6). There was a moderate, statistically significant correlation between degree of poration and fluorescence intensities in healthy samples (dorsal layer: $r = 0.34$ $p = 0.0116$,

intermediate layer: $r = 0.36$ $p = 0.0075$, ventral layer: $r = 0.42$, $p = 0.0014$). In fungal tissue, however, correlations were not statically significant.

## DISCUSSION

By visualizing the microscopic effects of ablative fractional $CO_2$ laser processing of nail tissue and quantitating ATTO-647N fluorescence intensity in healthy and fungal nail tissue, our study demonstrated that AFL-induced nail plate barrier disruptions can enhance the topical delivery of a small molecule (<900 g/mol).[46] The results of this preclinical investigation support the growing body of evidence on the clinical application of AFL pretreatment for enhanced efficacy of topical treatment of OM as summarized in Table 1.

Laser–tissue effects in healthy nail plates have previously been investigated using electron microscopy to characterize the ablation crater.[47,48] Our SEM assessment of the effects of a $CO_2$ laser, the most commonly employed device in LAUD studies, was consistent with previous reports of microscopic openings following AFL processing,[37] describing the efficient poration of the nail plate and creation of highly porous ablation crater surfaces. CARS-M visualized a thermal coagulation zone with strong autofluorescent signal associated with protein denaturation,[49] which was also visible on WFM, as well as a trilaminar nail plate structure characterized by its high water and lipid concentration in the intermediate layer. The increase in porosity and chemical composition of the nail plate layers may be part of the explanation for the mechanism behind LAUD.

Current evidence suggests that the typical thickening of the nail plate in OM is a compensatory reaction to its

**TABLE 2** Overview of morphometric microscopy measurements of nail tissue sections presented as means and standard deviations

| Sample | Number of samples (sections) | Nail thickness (SD) | Ablation depth (SD) | Degree of poration (SD) |
|---|---|---|---|---|
| ATTO-647N-labeled fungal nail with AFL | 6 (54) | 607 μm (163 μm) | 195 μm (59 μm) | 35% (16%) |
| ATTO-647N-labeled healthy nail with AFL | 6 (54) | 372 μm (75 μm) | 199 μm (56 μm) | 56% (21%) |
| Unlabeled healthy nail with AFL | 3 (27) | 450 μm (80 μm) | 163 μm (53 μm) | 38% (15%) |
| ATTO-647N-labeled fungal nail | 6 (54) | 572 μm (266 μm) | - | - |
| ATTO-647N-labeled healthy nail | 6 (54) | 487 μm (98 μm) | - | - |
| Unlabeled healthy nail | 3 (27) | 476 μm (143 μm) | - | - |

Abbreviations: AFL, ablative fractional laser; SD, standard deviation.

**FIGURE 3** Overlay of UV (grayscale) and ATTO-647N fluorescence (red pseudocolor) microscopy images of sections of intact and laser-processed nail tissue. Healthy nail shows modest diffusion of ATTO-647N seen primarily in the top layer (A), with a visible overall increase of signal intensity and wider distribution after fractional ablative laser treatment (B). In fungal nail tissue, ATTO-647N diffuses more easily into deeper layers (C) with increased signal intensity in the top layer after laser processing (D)
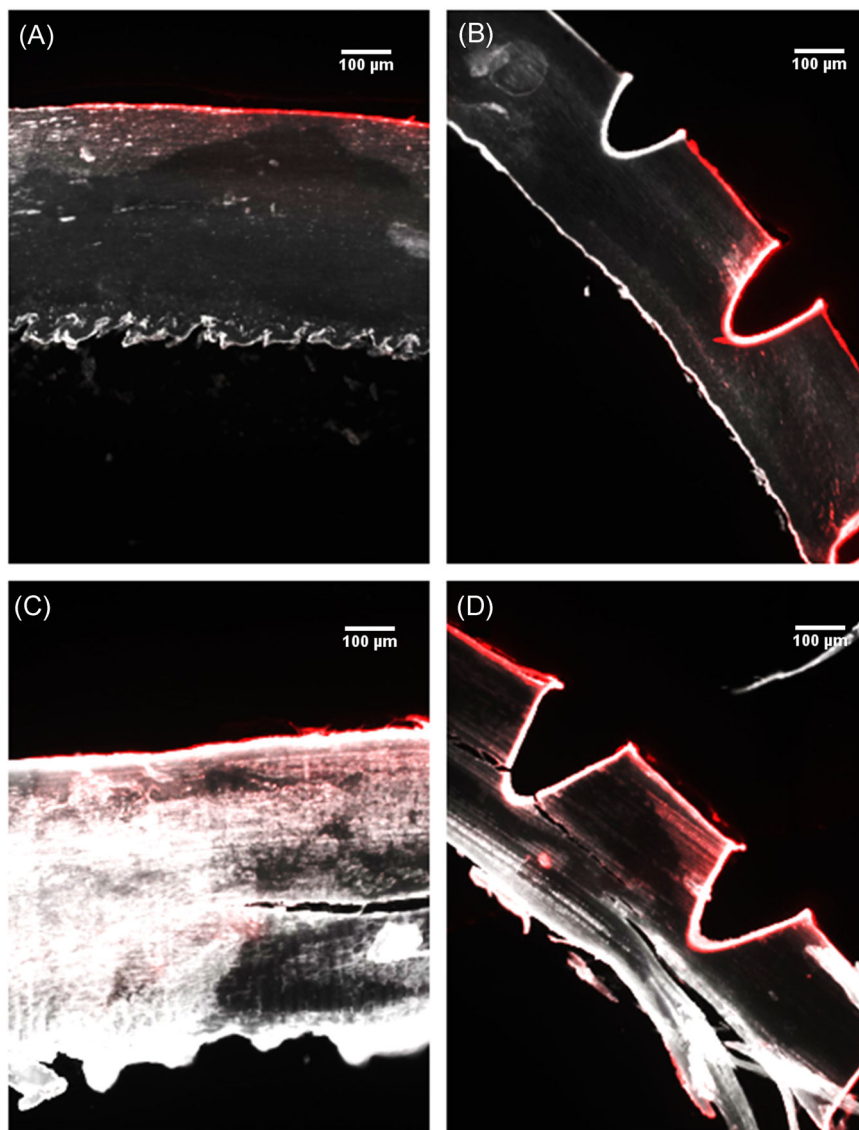


pathologically increased porosity to normalize the trans-onychial water loss.[50] In contrast to the tightly-packed nail layers of healthy nails with their brick-and-mortar-like cellular arrangement, WFM images of fungal nail samples displayed a distorted structure with gaps and fissures corresponding to signs of clinical nail dystrophy. Since the concept of LAUD is to physically disrupt and thereby overcome barriers to topical drug delivery, our

**TABLE 3** Overview of the average nail plate ATTO-647N fluorescence signal intensity (values in arbitrary units)

| Sample | Number of samples (sections) | Mean | SD | Median | MAD | Minimum | Maximum | Range | IQR |
|---|---|---|---|---|---|---|---|---|---|
| ATTO-647N-labeled fungal nail | 6 (54) | 305.4 | 307.5 | 167.7 | 92.0 | 102.1 | 1720.4 | 1618.3 | 228.0 |
| ATTO-647N-labeled healthy nail | 6 (54) | 146.3 | 68.6 | 117.1 | 20.4 | 100.8 | 502.2 | 401.5 | 48.2 |
| ATTO-647N-labeled fungal nail with AFL | 6 (54) | 428.1 | 421.8 | 273.8 | 195.2 | 102.2 | 2603.8 | 2501.5 | 324.9 |
| ATTO-647N-labeled healthy nail with AFL | 6 (54) | 308.2 | 248.8 | 202.0 | 128.0 | 102.3 | 1564.1 | 1461.8 | 270.7 |
| Unlabeled healthy nail | 3 (27) | 102.2 | 0.5 | 102.1 | 0.5 | 101.4 | 103.3 | 1.9 | 0.6 |
| Unlabeled healthy nail with AFL | 3 (27) | 103.2 | 1.0 | 103.0 | 1.0 | 101.7 | 106.6 | 4.9 | 1.3 |

Abbreviations: IQR, interquartile range; MAD, median absolute deviation; SD, standard deviation.

**TABLE 4** Pairwise comparison of ATTO-647N fluorescence signal intensities using Wilcoxon rank-sum test with continuity correction (Hochberg $p$ value adjustment)

| Samples | ATTO-647N-labeled fungal nail | ATTO-647N-labeled healthy nail | ATTO-647N-labeled fungal nail with AFL | ATTO-647N-labeled healthy nail with AFL |
|---|---|---|---|---|
| ATTO-647N-labeled fungal nail | | <0.0001 | <0.0001 | <0.0001 |
| ATTO-647N-labeled healthy nail | <0.0001 | | <0.0001 | <0.0001 |
| ATTO-647N-labeled fungal nail with AFL | <0.0001 | <0.0001 | | <0.0001 |
| ATTO-647N-labeled healthy nail with AFL | 0.09 | <0.0001 | <0.0001 | |

results show that AFL-pretreatment of healthy nail tissue leads to a larger increase in permeation than in already impaired fungal nail samples. This finding is in line with the results from a study on laser-assisted drug delivery in atopic dermatitis, demonstrating that barrier-deficient skin benefits from microporation though to a lesser degree than intact skin.[51] Other types of nail disorders, such as psoriatic nail disease, may present with similar clinical features but exhibit different micromorphologic changes and lower increase in porosity which could make them better targets for LAUD.[52,53] Since previous preclinical LAUD studies used healthy instead of diseased nail tissue, their results should be interpreted with caution as pretreatment effects for delivery enhancement may be overestimated.

Despite the paucity of preclinical studies of LAUD, several clinical trials have investigated the technique's potential for the treatment of OM and other nail disorders. Various AFL treatment regimens and parameters have been successfully combined with different formulations of low-molecular-weight compounds of <500 g/mol that can (Table 1). With a MW of 746 g/mol, ATTO-647N is more than twice as large as conventionally used antifungal agents (MW of terbinafine: 291.4 g/mol) and exceeds the '500 Dalton rule' for optimal cutaneous penetration,[54] suggesting that low MW may not be critical to LAUD.[55] An earlier study made by Vanstone et al. on AFL-enhanced delivery of topically applied aqueous caffeine solution (MW = 194.2 g/mol) found the degree

of poration to be an important factor in the delivery enhancement.[47] In line with their results, our study found a correlation between the degree of poration and fluorescence signal intensity. However, this association was more pronounced in healthy tissue, suggesting that lower pulse energy may be sufficient to enhance drug distribution in diseased nail plates. Previous imaging investigations of the effects of AFL on nail tissue indicate that optical coherence tomography (OCT) is a reliable noninvasive method to detect variation in micropore dimensions and nail plate thickness.[45,56] By incorporating OCT, LAUD for nail disease could be optimized and adjusted to the clinical presentation by tailoring the pulse energy to achieve sufficient poration for optimal drug delivery enhancement depending on the extent of the fungal infection.

Limitations of this study are the lack of information on the specific fungal subtyping and the substantial variation in nail plate poration. Given the ex vivo design, our results cannot be used to draw clinical conclusions on the efficacy and safety of LAUD in patients with OM. While determining the fungal pathogen is critical for efficacious treatment, microstructural alterations of the nail plate and their impact on the barrier function are common for all types of fungal infections. Inconsistency in nail plate poration despite standardized device settings has previously been reported and is thought to be due to non-perpendicular laser beam impact. While clippings can
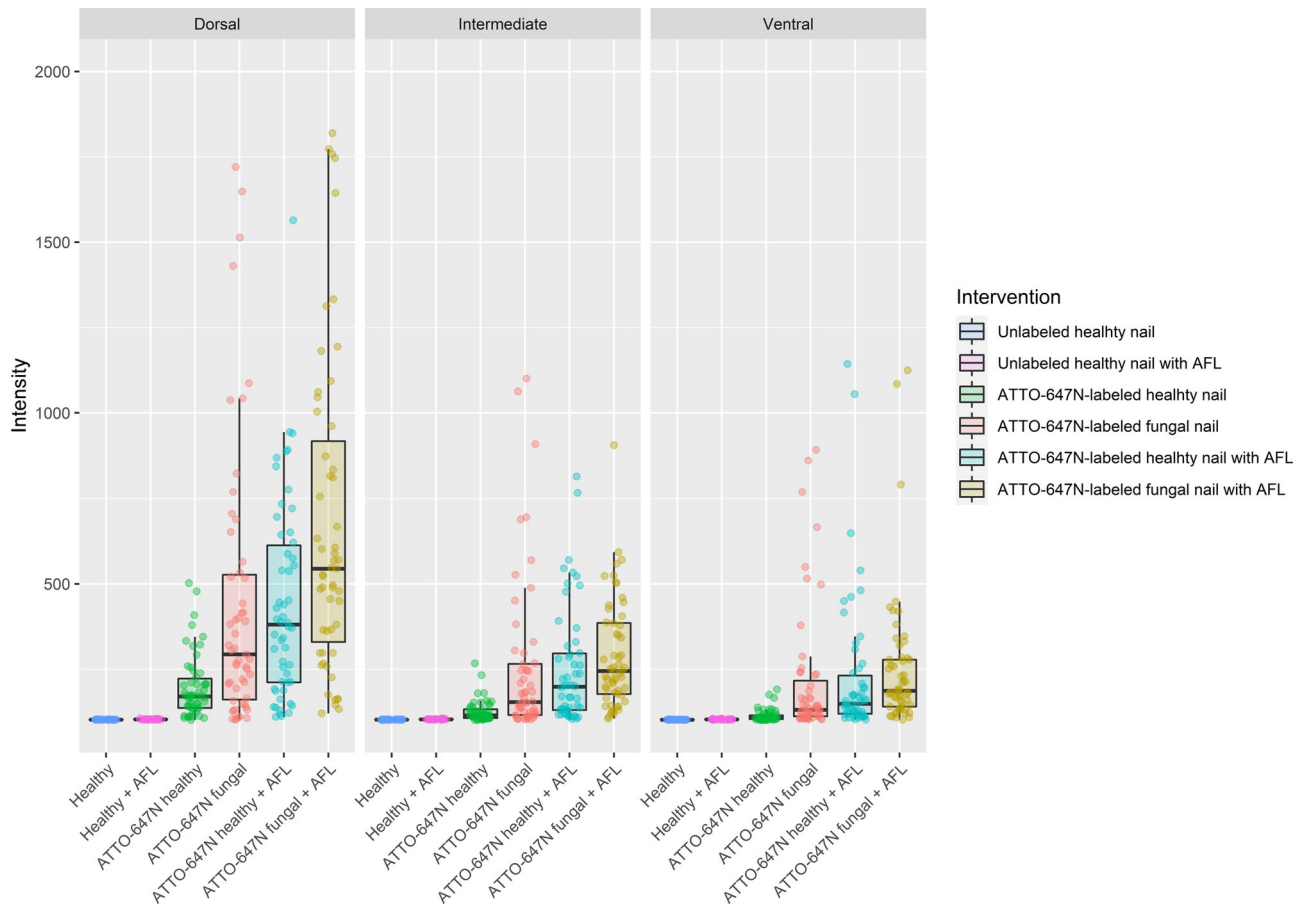
**FIGURE 4** Faceted boxplot showing ATTO-647N fluorescence intensities measured in the dorsal, intermediate, and ventral portion of healthy and fungal nail samples with and without ablative fractional laser pretreatment

**TABLE 5** Mean ATTO-647N fluorescence signal intensities (values in arbitrary units) for each nail plate layer.

| Nail plate layer | Unlabeled healthy nail | Unlabeled healthy nail with AFL | ATTO-647N-labeled healthy nail | ATTO-647N-labeled healthy nail with AFL | ATTO-647N-labeled fungal nail | ATTO-647N-labeled fungal nail with AFL |
|---|---|---|---|---|---|---|
| Top layer | 102.2 | 103.2 | 198.7 | 442.0 | 448.3 | 758.9 |
| Middle layer | 102.2 | 103.3 | 126.2 | 252.0 | 254.8 | 294.9 |
| Bottom layer | 102.1 | 103.0 | 114.0 | 230.6 | 216.4 | 243.5 |

**TABLE 6** Percentage change of ATTO-647N fluorescence signal intensity in healthy and fungal ex vivo nail tissue

| Nail plate layer | Increase in healthy nail after AFL | Increase in fungal nail after AFL | Increase in signal due to infection (healthy vs. fungal) |
|---|---|---|---|
| Top layer | +122% | +69% | +126% |
| Middle layer | +100% | +16% | +102% |
| Bottom layer | +102% | +13% | +90% |
| Average | +108% | +33% | +106% |

be trimmed to flatten the curvature of the nail, variation in microporation is to be expected when implementing LAUD in a clinical setting. Flattening the nail plate using a $CO_2$-laser transmissive optical window made of zinc selenide could present a convenient alternative that merits further investigation.[57]

The current treatment paradigm for OM rests on pharmacological management with either topically or

orally administered antifungal agents. While laser therapy of OM has only been cleared by the US Food and Drug Administration (FDA) for "temporary increase in clear nail,"[58] in-office laser treatments may prove beneficial for patients where medication adherence or systemic interactions are a concern. Given the low cure rate of approved treatment options (Table S1), off-label treatment using LAUD of topical agents may represent an alternative for patients not tolerating or not responding to conventional approaches.[59] Despite already promising meta-analytic evidence on LAUD in clinical practice,[60] identification of predictive factors for treatment response, such as dystrophic changes of the nail plate, is warranted.

In this study, we demonstrated that AFL-processing causes micromorphologic changes that may explain the increased delivery of an aqueous solution after four hours of incubation in both healthy and damaged nail plates, supporting the results of clinical trials on LAUD for the treatment of nail disease. Nail dystrophy and its impact on the barrier function of the nail appear to be critical factors in determining the permeability and aptness of nail tissue for LAUD. More studies are needed to assess the kinetic relationship of LAUD in diseased nails, the benefit of repeated topical application of the compound, and the impact of vehicle formulations to evaluate their compatibility with this delivery technique.

# CONCLUSION

Microporation of nail tissue using a fractional $CO_2$ laser is a simple yet effective way of enhancing the delivery of a topically applied solution. Although dystrophic changes of the fungal nail plate structure lead to increased permeability, both structurally deficient and intact nails appear to benefit from laser pretreatment for ungual delivery.

## AUTHOR CONTRIBUTIONS

*Study conception and design*: Vinzent Kevin Ortner, Jonathan R. Brewer, Merete Haedersdal, and Peter Alshede Philipsen. *Acquisition of data*: Vinzent Kevin Ortner, Nhi Nguyen, and Vita Solovyeva. *Analysis and interpretation of data*: Vinzent Kevin Ortner, Nhi Nguyen, and Peter Alshede Philipsen. *Drafting of manuscript*: Vinzent Kevin Ortner, Nhi Nguyen. *Critical revision*: Merete Haedersdal, Jonathan R. Brewer, Vita Solovyeva, and Peter Alshede Philipsen.

## ORCID
*Vinzent Kevin Ortner* https://orcid.org/0000-0001-9708-6717
*Jonathan R. Brewer* http://orcid.org/0000-0002-3444-1715
*Merete Haedersdal* http://orcid.org/0000-0003-1250-2035
*Peter Alshede Philipsen* http://orcid.org/0000-0002-9656-733X

## REFERENCES

1. Lipner SR, Scher RK. Management of onychomycosis and co-existing tinea pedis. J Drugs Dermatol. 2015;14:492–4. http://jddonline.com/articles/dermatology/S1545961615P0492X/1
2. Yeung K, Ortner VK, Martinussen T, Paasch U, Haedersdal M. Efficacy of laser treatment for onychomycotic nails: a systematic review and meta-analysis of prospective clinical trials. Lasers Med Sci. 2019;34(8):1513–25. https://doi.org/10.1007/s10103-019-02802-8
3. Lipner SR, Scher RK. Part I: onychomycosis: clinical overview and diagnosis. J Am Acad Dermatol. 2018;80:835–51. https://doi.org/10.1016/j.jaad.2018.03.062
4. Warshaw EM, Foster JK, Cham PMH, Grill JP, Chen SC. NailQoL: a quality-of-life instrument for onychomycosis. Int J Dermatol. 2007;46(12):1279–86. https://doi.org/10.1111/j.1365-4632.2007.03362.x
5. Saunte DM, Holgersen JB, Haedersdal M, Strauss G, Bitsch M, Svendsen OL, et al. Prevalence of toe nail onychomycosis in diabetic patients. Acta Derm Venereol. 2006;86(5):425–8. https://doi.org/10.2340/00015555-0113
6. Gupta AK, Mays RR. The impact of onychomycosis on quality of life: a systematic review of the available literature. Skin Appendage Disord. 2018;4(4):208–16. https://doi.org/10.1159/000485632
7. Roujeau JC, Sigurgeirsson B, Korting HC, Kerl H, Paul C. Chronic dermatomycoses of the foot as risk factors for acute bacterial cellulitis of the leg: a case-control study. Dermatology. 2004;209(4):301–7. https://doi.org/10.1159/000080853
8. Lipner SR, Scher RK. Onychomycosis: clinical overview and diagnosis. J Am Acad Dermatol. 2019;80(4):835–51. https://doi.org/10.1016/j.jaad.2018.03.062
9. Kreijkamp-Kaspers S, Hawke K, Guo L, Kerin G, Bell-Syer SE, Magin P, et al. Oral antifungal medication for toenail onychomycosis. Cochrane Database Syst Rev. 2017;7:CD010031. https://doi.org/10.1002/14651858.CD010031.pub2
10. Wenande E, Erlendsson AM, Haedersdal M. Opportunities for laser-assisted drug delivery in the treatment of cutaneous disorders. Semin Cutan Med Surg. 2017;36(4):192–201. https://doi.org/10.12788/j.sder.2017.046
11. Chiu WS, Belsey NA, Garrett NL, Moger J, Delgado-Charro MB, Guy RH. Molecular diffusion in the human nail measured by stimulated Raman scattering microscopy. Proc Natl Acad Sci U S A. 2015;112(25):7725–30. https://doi.org/10.1073/pnas.1503791112
12. Nguyen HX, Banga AK. Effect of ablative laser on in vitro transungual delivery. Int J Pharm. 2018;544(2):402–14. https://doi.org/10.1016/j.ijpharm.2017.09.048
13. Vanstone S, Cordery SF, Stone JM, Gordeev SN, Guy RH. Precise laser poration to control drug delivery into and through human nail. J Control Release. 2017;268:72–7. https://doi.org/10.1016/j.jconrel.2017.10.014
14. Lim EH, Seo YJ, Lee JH, Im M. Onychodystrophy treated using fractional carbon dioxide laser therapy and topical steroids: new

treatment options for nail dystrophy. Dermatol Surg. 2013;39(12): 1931–3. https://doi.org/10.1111/dsu.12365

15. Morais OO, de, Costa IMC, Gomes CM, Shinzato DH, Ayres GMC, Cardoso RM. The use of the Er:YAG 2940nm laser associated with amorolfine lacquer in the treatment of onychomycosis. An Bras Dermatol. 2013;88(5):847–9. https://doi.org/10.1590/abd1806-4841.20131932

16. Lim EH, Kim HR, Park YO, Lee Y, Seo YJ, Kim CD, et al. Toenail onychomycosis treated with a fractional carbon-dioxide laser and topical antifungal cream. J Am Acad Dermatol. 2014; 70(5):918–23. https://doi.org/10.1016/j.jaad.2014.01.893

17. de Oliveira GB, Antonio JR, Antonio CR, Tomé FA. The association of fractional CO2 laser 10.600nm and photodynamic therapy in the treatment of onychomycosis. An Bras Dermatol. 2015;90(4):468–71. https://doi.org/10.1590/abd1806-4841.20153588

18. Bhatta AK, Keyal U, Huang X, Zhao JJ. Fractional carbon-dioxide (CO2) laser-assisted topical therapy for the treatment of onychomycosis. J Am Acad Dermatol. 2016;74(5):916–23. https://doi.org/10.1016/j.jaad.2015.12.002

19. Zhou BR, Lu Y, Permatasari F, Huang H, Li J, Liu J, et al. The efficacy of fractional carbon dioxide (CO2) laser combined with luliconazole 1% cream for the treatment of onychomycosis: a randomized, controlled trial. Medicine. 2016;95(44):e5141. https://doi.org/10.1097/MD.0000000000005141

20. Zhang J, Lu S, Huang H, Li X, Cai W, Ma J, et al. Combination therapy for onychomycosis using a fractional 2940-nm Er:YAG laser and 5% amorolfine lacquer. Lasers Med Sci. 2016;31(7): 1391–6. https://doi.org/10.1007/s10103-016-1990-z

21. Shi J, Li J, Huang H, Permatasari F, Liu J, Xu Y, et al. The efficacy of fractional carbon dioxide (CO2) laser combined with terbinafine hydrochloride 1% cream for the treatment of onychomycosis. J Cosmet Laser Ther. 2017;19(6):353–9. https://doi.org/10.1080/14764172.2017.1334925

22. Koren A, Salameh F, Sprecher E, Artzi O. Laser-assisted photodynamic therapy or laser-assisted amorolfine lacquer delivery for treatment of toenail onychomycosis: an open-label comparative study. Acta Derm Venereol. 2018;98(4):467–8. https://doi.org/10.2340/00015555-2874

23. Abd El-Aal EB, Abdo HM, Ibrahim SM, Eldestawy MT. Fractional carbon dioxide laser assisted delivery of topical tazarotene versus topical tioconazole in the treatment of onychomycosis. J Dermatol Treat. 2019;30(3):277–82. https://doi.org/10.1080/09546634.2018.1509046

24. El-Tatawy RA, Aliweh HA, Hegab DS, Talaat RAZ, Shams Eldeen MA. Fractional carbon dioxide laser and topical tioconazole in the treatment of fingernail onychomycosis. Lasers Med Sci. 2019;34(9):1873–80. https://doi.org/10.1007/s10103-019-02789-2

25. Abdallah M, Abu-Ghali MM, El-Sayed MT, Soltan MY. Fractional CO2-assisted photodynamic therapy improves the clinical outcome and patient's satisfaction in toenail onychomycosis treatment: an intra-patient comparative single-center study. J Dermatol Treat. 2022;33:542–9. https://doi.org/10.1080/09546634.2020.1771252

26. Rajbanshi B, Shen L, Jiang M, Gao Q, Huang X, Ma J, et al. Comparative study of traditional ablative CO2 laser-assisted topical antifungal with only topical antifungal for treating onychomycosis: a multicenter study. Clin Drug Investig. 2020; 40(6):575–82. https://doi.org/10.1007/s40261-020-00914-6

27. Zaki AM, Abdo HM, Ebadah MA, Ibrahim SM. Fractional CO2 laser plus topical antifungal versus fractional CO2 laser versus topical antifungal in the treatment of onychomycosis. Dermatol Ther. 2020;33:e13155. https://doi.org/10.1111/dth.13155

28. Zhang J, Zhang Y, Qin J, Lu S, Cai W, Li J, et al. Comparison of a fractional 2940-nm Er:YAG laser and 5% amorolfine lacquer combination therapy versus a 5% amorolfine lacquer monotherapy for the treatment of onychomycosis: a randomized controlled trial. Lasers Med Sci. 2021;36(1):147–52. https://doi.org/10.1007/s10103-020-03054-7

29. Shehadeh W, Matz H, Ellenbogen E, Sprecher E, Artzi O. Pulse-dye laser followed by betamethasone-calcipotriol and fractional ablative CO2-laser-assisted delivery for nail psoriasis. Dermatol Surg. 2021; 47(4):111–6. https://doi.org/10.1097/DSS.0000000000002835

30. Essa Abd Elazim N, Mahmoud Abdelsalam A, Mohamed Awad S. Efficacy of combined fractional carbon dioxide laser and topical tazarotene in nail psoriasis treatment: a randomized intrapatient left-to-right study. J Cosmet Dermatol. Published online October 19, 2021. https://doi.org/10.1111/jocd.14536

31. Yang CH, Tsai MT, Shen SC, Ng CY, Jung SM. Feasibility of ablative fractional laser-assisted drug delivery with optical coherence tomography. Biomed Opt Express. 2014;5(11): 3949–59. https://doi.org/10.1364/BOE.5.003949

32. Tsai MT, Tsai TY, Shen SC, Ng CY, Lee YJ, Lee JD, et al. Evaluation of laser-assisted trans-nail drug delivery with optical coherence tomography. Sensors. 2016;16(12):2111. https://doi.org/10.3390/s16122111

33. Belikov AV, Tavalinskaya AD, Smirnov SN, Sergeev AN. Active Er-laser drug delivery using drug-impregnated gel for treatment of nail diseases. Biomed Opt Express. 2019;10(7):3232–40. https://doi.org/10.1364/BOE.10.003232

34. Šveikauskaitė I, Pockevičius A, Briedis V. Potential of chemical and physical enhancers for transungual delivery of amorolfine hydrochloride. Materials. 2019;12(7):1028. https://doi.org/10.3390/ma12071028

35. Šveikauskaitė I, Briedis V. Potential of naftifine application for transungual delivery. Molecules. 2020;25(13):3043. https://doi.org/10.3390/molecules25133043

36. Belikov AV, Tavalinskaya AD, Smirnov SN. Investigation of the dual-stage method of active Er:YLF laser drug delivery through the nail and laser-induced transformations of the drug extinction spectrum. Lasers Surg Med. 2021;53:1122–31. https://doi.org/10.1002/lsm.23379

37. Vanstone S, Stone JM, Gordeev SN, Guy RH. Mechanism of human nail poration by high-repetition-rate, femtosecond laser ablation. Drug Deliv Transl Res. 2019;9(5):956–67. https://doi.org/10.1007/s13346-019-00638-x

38. D.p W, M.j V. Onychomycosis: current trends in diagnosis and treatment. Am Fam Physician. 2013;88:762–70.

39. Farren L, Shayler S, Ennos AR. The fracture properties and mechanical design of human fingernails. J Exp Biol. 2004;207(5): 735–41. https://doi.org/10.1242/jeb.00814

40. Nguyen JNT, Harbison AM. Scanning electron microscopy sample preparation and imaging. Methods Mol Biol. 2017;1606: 71–84. https://doi.org/10.1007/978-1-4939-6990-6_5

41. Coherent Anti-Stokes Raman Scattering Microscopy: Chemical Imaging for Biology and Medicine | Annual Review of Analytical Chemistry. Accessed January 7, 2019. https://www.annualreviews.org/doi/abs/10.1146/annurev.anchem.1.031207.112754?rfr_dat=cr_pub%3Dpubmed&url_ver=Z39.88-2003&rfr_id=ori%3Arid%3Acrossref.org&journalCode=anchem

42. Thorsted B, Bloksgaard M, Groza A, Schousboe LP, Færgeman NJ, Sørensen JA, et al. Biochemical and bioimaging evidence of cholesterol in acquired cholesteatoma. Ann Otol Rhinol Laryngol. 2016;125(8):627–33. https://doi.org/10.1177/0003489416642784

43. Iachina I, Antonescu IE, Dreier J, Sørensen JA, Brewer JR. The nanoscopic molecular pathway through human skin. Biochim Biophys Acta BBA - Gen Subj. 2019;1863(7):1226–33. https://doi.org/10.1016/j.bbagen.2019.04.012

44. Schindelin J, Arganda-Carreras I, Frise E, Kaynig V, Longair M, Pietzsch T, et al. Fiji: an open-source platform for biological-image analysis. Nat Methods. 2012;9(7):676–82. https://doi.org/10.1038/nmeth.2019

45. Ortner VK, Holmes J, Haedersdal M, Philipsen PA. Morphometric optical imaging of microporated nail tissue: an investigation of intermethod agreement, reliability, and technical limitations. Lasers Surg Med. 2020;53:838–48. https://doi.org/10.1002/lsm.23304

46. Small-Molecule Inhibitors of the Receptor Tyrosine Kinases: Promising Tools for Targeted Cancer Therapies. Accessed July 24, 2021. https://www-ncbi-nlm-nih-gov.ep.fjernadgang.kb.dk/pmc/articles/PMC4159824/

47. Vanstone S, Cordery SF, Stone JM, Gordeev SN, Guy RH. Precise laser poration to control drug delivery into and through human nail. J Controlled Release. 2017;268:72–7. https://doi.org/10.1016/j.jconrel.2017.10.014

48. Neev J, Nelson JS, Critelli M, McCullough JL, Cheung E, Carrasco WA, et al. Ablation of human nail by pulsed lasers. Lasers Surg Med. 1997;21(2):186–92. https://doi.org/10.1002/(SICI)1096-9101(1997)21:2<186::AID-LSM10>3.0.CO;2-D

49. Hennings L, Kaufmann Y, Griffin R, Siegel E, Novak P, Corry P, et al. Dead or alive? Autofluorescence distinguishes heat-fixed from viable cells. Int J Hyperth. 2009;25(5):355–63. https://doi.org/10.1080/02656730902964357

50. McAuley WJ, Jones SA, Traynor MJ, Guesné S, Murdan S, Brown MB. An investigation of how fungal infection influences drug penetration through onychomycosis patient's nail plates. Eur J Pharm Biopharm. 2016;102:178–84. https://doi.org/10.1016/j.ejpb.2016.03.008

51. Lee WR, Shen SC, Sung CT, Liu PY, Fang JY. Is the fractional laser still effective in assisting cutaneous macromolecule delivery in barrier-deficient skin? Psoriasis and atopic dermatitis as the disease models. Pharm Res. 2018;35(7):128. https://doi.org/10.1007/s11095-018-2413-6

52. Cutrín Gómez E, Anguiano Igea S, Delgado-Charro MB, Gómez Amoza JL, Otero Espinar FJ. Microstructural alterations in the onychomycotic and psoriatic nail: relevance in drug delivery. Eur J Pharm Biopharm. 2018;128:48–56. https://doi.org/10.1016/j.ejpb.2018.04.012

53. G.k L, M H, E.l S. The prevalence of onychomycosis in patients with psoriasis and other skin diseases. Acta Derm Venereol. 2003;83:206–9.

54. Bos JD, Meinardi MM. The 500 Dalton rule for the skin penetration of chemical compounds and drugs. Exp Dermatol. 2000;9(3):165–9. https://doi.org/10.1034/j.1600-0625.2000.009003165.x

55. Davies-Strickleton H, Cook J, Hannam S, Bennett R, Gibbs A, Edwards D, et al. Assessment of the nail penetration of antifungal agents, with different physico-chemical properties. PLoS One. 2020;15(2):e0229414. https://doi.org/10.1371/journal.pone.0229414

56. Ortner VK, Mandel VD, Haedersdal M, Philipsen PA. Impregnation of healthy nail tissue with optical clearing agents for improved optical coherence tomography imaging. Skin Res Technol. 2021;27(2):178–82. https://doi.org/10.1111/srt.12923

57. Moore BA, Daamen N, Biesman BS, Reinisch L. Carbon dioxide laser skin resurfacing with a cooled handpiece. Lasers Surg Med. 2001;29(3):236–43. https://doi.org/10.1002/lsm.1113

58. Gupta AK, Foley KA, Versteeg SG. Lasers for onychomycosis. J Cutan Med Surg. 2017;21(2):114–6. https://doi.org/10.1177/1203475416677722

59. Gupta AK, Stec N. Recent advances in therapies for onychomycosis and its management. F1000Research. 2019;8:968. https://doi.org/10.12688/f1000research.18646.1

60. Han Y, Wang Y, Zhang X, Chen J, Li XD. The effects of CO2 laser and topical agent combination therapy for onychomycosis: a meta-analysis. Dermatol Ther. 2021;34(6):e15136. https://doi.org/10.1111/dth.15136

## SUPPORTING INFORMATION

Additional supporting information can be found online in the Supporting Information section at the end of this article.

---

**How to cite this article:** Ortner VK, Nguyen N, Brewer JR, Solovyeva V, Haedersdal M, Philipsen PA. Fractional $CO_2$ laser ablation leads to enhanced permeation of a fluorescent dye in healthy and mycotic nails—An imaging investigation of laser–tissue effects and their impact on ungual drug delivery. Lasers Surg Med. 2022;54:861–874.

https://doi.org/10.1002/lsm.23541